Developmental Cell
Article

High-Resolution Temporal Analysis Reveals a Functional Timeline for the Molecular Regulation of Cytokinesis

Tim Davies,[1,7] Shawn N. Jordan,[1,7] Vandana Chand,[1] Jennifer A. Sees,[2] Kimberley Laband,[3] Ana X. Carvalho,[4] Mimi Shirasu-Hiza,[5] David R. Kovar,[2,6] Julien Dumont,[3] and Julie C. Canman[1,*]
[1]Department of Pathology and Cell Biology, Columbia University, New York, NY 10032, USA
[2]Department of Molecular Genetics and Cell Biology, University of Chicago, Chicago, IL 60637, USA
[3]CNRS, Institut Jacques Monod, Univ. P7, 75205 Paris CEDEX 13, France
[4]Molecular and Cellular Biology Unit, Instituto de Biologia Molecular e Celular (IBMC), 4150-180 Porto, Portugal
[5]Department of Genetics and Development, Columbia University, New York, NY 10032, USA
[6]Department of Biochemistry and Molecular Biology, University of Chicago, Chicago, IL 60637, USA
[7]Co-first author
*Correspondence: jcc2210@columbia.edu
http://dx.doi.org/10.1016/j.devcel.2014.05.009

SUMMARY

To take full advantage of fast-acting temperature-sensitive mutations, thermal control must be extremely rapid. We developed the Therminator, a device capable of shifting sample temperature in ~17 s while simultaneously imaging cell division in vivo. Applying this technology to six key regulators of cytokinesis, we found that each has a distinct temporal requirement in the *Caenorhabditis elegans* zygote. Specifically, myosin-II is required throughout cytokinesis until contractile ring closure. In contrast, formin-mediated actin nucleation is only required during assembly and early contractile ring constriction. Centralspindlin is required to maintain division after ring closure, although its GAP activity is only required until just prior to closure. Finally, the chromosomal passenger complex is required for cytokinesis only early in mitosis, but not during metaphase or cytokinesis. Together, our results provide a precise functional timeline for molecular regulators of cytokinesis using the Therminator, a powerful tool for ultra-rapid protein inactivation.

INTRODUCTION

The field of cell biology has been greatly advanced by the assembly of "parts lists" of molecules required for complex cellular behaviors such as cell motility and cell division. With parts lists in hand, we must now begin to understand how these molecular pathways cooperate spatially and temporally to execute cell behavior.

Cytokinesis, the physical division of one cell into two daughter cells, provides a clear example of the complexity of spatiotemporal regulation. Upon initiation of chromosome segregation in anaphase, an antiparallel array of microtubules, known as the central spindle, forms between the separating chromosomes. Signals originating from the central spindle and spindle asters then activate the assembly and constriction of an actomyosin contractile ring between the chromosomes to divide the cell into two (Green et al., 2012).

Three known spindle-associated signaling pathways regulate cytokinesis: the RhoA, Rac1, and the chromosomal passenger complex (CPC) pathways (Figure 1A). In the RhoA-mediated activation pathway, the spindle targets the guanine nucleotide exchange factor (GEF) ECT-2 to the cell cortex at the division plane (Su et al., 2011; Yüce et al., 2005; Zhao and Fang, 2005), where ECT-2 triggers RhoA to exchange GDP for GTP (Kimura et al., 2000). Activated, GTP-bound RhoA then stimulates contractile ring assembly and constriction at the division plane by increasing both linear F-actin polymerization via the nucleator formin^{CYK-1} and myosin-II^{NMY-2} motor activity (Green et al., 2012). In the Rac1-mediated pathway, active GTP-bound Rac1 inhibits actomyosin-driven contractile ring constriction at the plasma membrane (Bastos et al., 2012). Thus, for cytokinesis to occur, the regulatory complex centralspindlin is targeted to the central spindle (Mishima et al., 2002), where it inactivates Rac1 at the division plane via its GTPase activating protein (GAP) domain (Bastos et al., 2012; Canman et al., 2008; Jordan and Canman, 2012; Yoshizaki et al., 2004). Finally, the CPC pathway (Lewellyn et al., 2011) is the least well understood in terms of its regulation of cytokinesis. The CPC localizes to the chromosomes throughout mitosis before "passenging" in anaphase to the central spindle and is required for full contractile ring constriction by an unknown mechanism (Carmena et al., 2012).

While all three pathways are important components of cytokinetic signaling, the precise temporal windows in which they act are unknown. This deficit stems in part from the fact that cytokinesis is quite rapid (~5–30 m from contractile ring assembly to closure). Furthermore, many of the proteins in these pathways play additional roles at other stages of the cell cycle, throughout oogenesis and organismal development, thus precluding traditional forward genetic approaches.

Conditional inactivation of proteins can provide valuable information about temporal requirements in specific processes. However, most methods take several minutes for

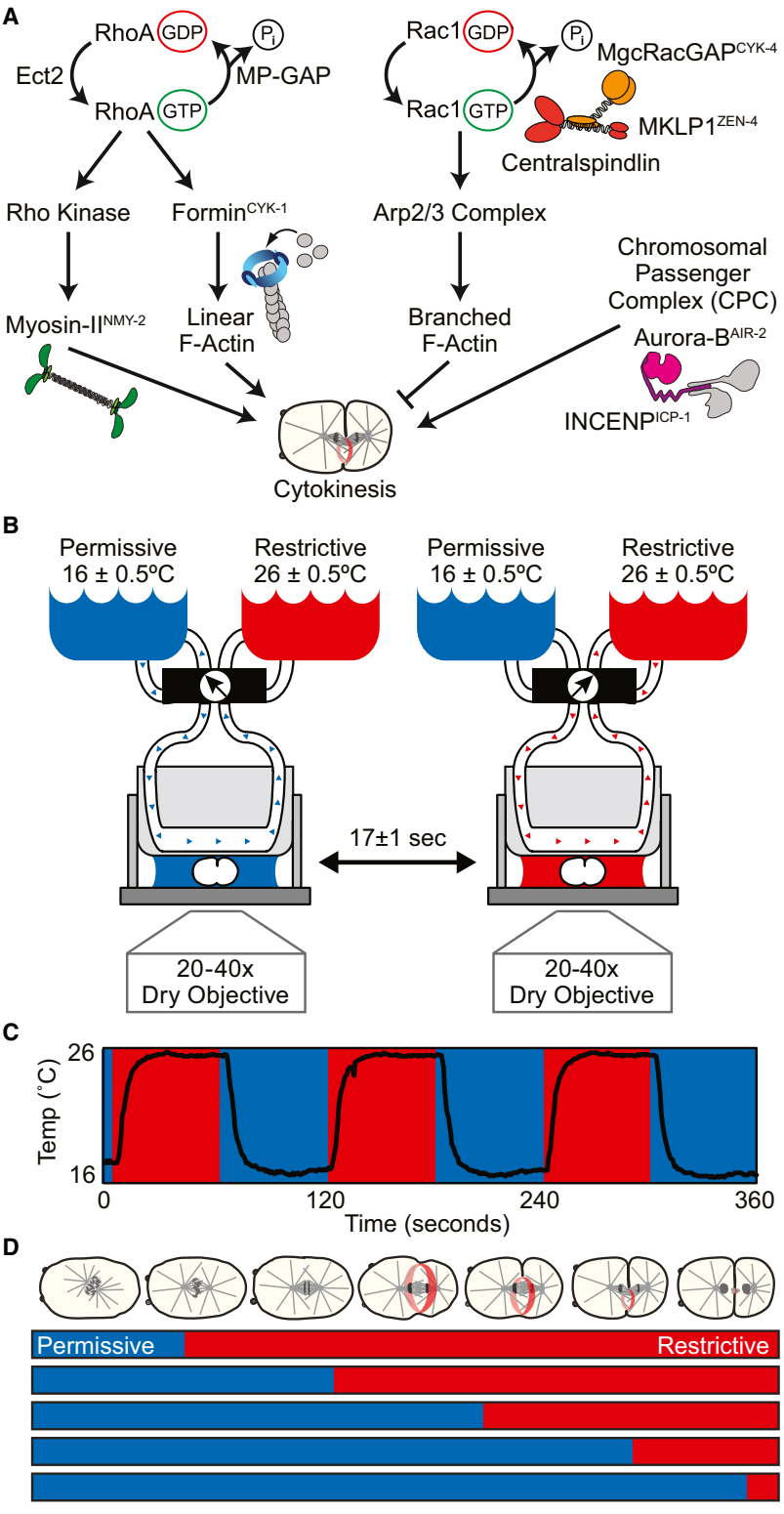

Figure 1. Approach to Understanding the Molecular Regulation of Cytokinesis at High Temporal Resolution

(A) The conserved molecular pathways essential for cytokinesis.

(B) Schematic representation of the Therminator.

(C) Graph showing the temperature of the Therminator specimen chamber over time. Switch between 16°C ± 0.5°C and 26°C ± 0.5°C is indicated by the change in background color.

(D) Schematic showing experimental protocol. The mounted ts mutant zygote is upshifted at a precise time point during cell division to determine the temporal window of activity required for cytokinesis. Blue, permissive; red, restrictive.

protein inactivation and are irreversible on short time scales (Nishimura et al., 2009; Robinson et al., 2010). In contrast, fast-acting temperature-sensitive (ts) mutations in the nematode *Caenorhabditis elegans* allow conditional and reversible disruption of protein function within seconds by simply shifting from permissive (16°C) to restrictive temperature (26°C; or vice versa) at the desired time point. This strategy has been used in previous studies of cytokinesis with ~60–70 s temporal resolution using differential interference contrast microscopy to score the progression of cytokinesis (Liu et al., 2010; Severson et al., 2000). However, cytokinesis in *Caenorhabditis elegans* occurs within ~500 s. Thus, faster resolution is essential to dissect the temporal roles of key regulators in the individual processes of contractile ring assembly, constriction, and closure.

Here we combine cytokinesis-defective, fast-acting ts mutants with a fluidic device called the Therminator that allows simultaneous rapid (~17 s) temperature shifts and live cell analysis. This has allowed us to define the precise temporal requirements for the three conserved molecular signaling pathways essential for regulating cytokinesis.

RESULTS

Rapid Control of Protein Function with the Therminator and Fast-Acting ts Mutants

To decrease the time required to inactivate ts protein function with temperature and take full advantage of fast-acting ts *C. elegans* mutants, we developed a fluidic device that we call the Therminator (Figure 1B). Using two water baths, one at permissive (16°C ± 0.5°C) and the other at restrictive temperature (26°C ± 0.5°C), the specimen chamber of the Therminator is stably maintained at the appropriate temperature until the desired time of shift (Figures 1B and 1C). When the source bath switch is triggered, the specimen is rapidly shifted to the new temperature (17 ± 1 s, n = 10; Figures 1B and 1C). The Therminator specimen chamber was also designed for optical clarity and compatibility with automatic focusing hardware. Thus, the Therminator permits rapid ts

protein inactivation while allowing for high-resolution imaging of the zygote by four-dimensional spinning disc confocal microscopy before, during, and after the temperature shift.

We used six cytokinesis-defective ts mutants that disrupt the function of conserved proteins in each of three key cytokinetic pathways (Figure 1A; Table S1 available online). For the RhoA pathway, which stimulates actomyosin dynamics, we used ts mutations in myosin-II^{NMY-2} and the actin nucleator formin^{CYK-1}. For the Rac1 pathway, we used ts mutations that affect both components of the centralspindlin complex: MKLP1^{ZEN-4} and MgcRacGap^{CYK-4}. Finally, for the CPC pathway, we used ts mutations in two components of this complex: INCENP^{ICP-1} and Aurora-B^{AIR-2} kinase. Four of these mutants have been previously published, while two (*formin^{CYK-1}(ts)* and *INCENP^{ICP-1}(ts)*) are novel alleles identified in a screen for cytokinesis-defective ts mutants (Canman et al., 2008). All ts mutations were introduced into strains expressing an mCherry::Histone-H2B fusion to label the chromosomes and a GFP::PH fusion to label the plasma membrane. These labels facilitate the accurate analysis of the kinetics of cleavage furrow onset, contractile ring constriction, and ring closure, while at the same time monitoring the underlying cell cycle events.

We first used the Therminator to confirm that these ts alleles are both fast-acting and reversible (Figure S1). For each allele, zygotes upshifted early in the first mitosis and maintained at the restrictive temperature showed the full loss-of-function phenotype (Figure S1A). In each case, activity of the ts protein could be rapidly restored, such that cytokinesis was completed, by downshifting prior to the earliest cell division event in which each individual protein is known to be required (Figure S1B). For example, *formin^{CYK-1}(ts)* zygotes were upshifted at nuclear envelope breakdown and then downshifted just prior to anaphase onset (held for ~180 s at 26°C ± 0.5°C). Despite the period of early upshift, *formin^{CYK-1}(ts)* zygotes divided successfully when returned to 16°C ± 0.5°C. Thus, each ts mutation is fast acting and reversible (Figure S1). We next used the Therminator to systematically induce protein inactivation at specific points during cell division (Figure 1D and Supplemental Experimental Procedures).

The RhoA Pathway and Actomyosin Dynamics

Myosin-II^{NMY-2} Activity Is Required until Contractile Ring Closure but Is Partially Dispensable for Constriction

To study the temporal contribution of myosin-II^{NMY-2} during cytokinesis, we used a fast-acting *myosin-II^{NMY-2}(ts)* allele with an L981P substitution within the S2 region (Liu et al., 2010) (Figure 2A; Table S1). This point mutation is predicted to disrupt the S2 coiled-coil structure (COILS program; Lupas et al., 1991) involved in dimerization and head-head coupling (Tama et al., 2005). Metaphase upshift of *myosin-II^{NMY-2}(ts)* zygotes prevented the initiation of furrowing and caused cytokinesis failure, replicating the full *myosin-II^{NMY-2}* loss-of-function phenotype (Figure S1). Despite failing to initiate a furrow, a fluorescent F-actin reporter, GFP::Utrophin^{ABD} (Tse et al., 2012), revealed that *myosin-II^{NMY-2}(ts)* zygotes were still able to localize F-actin to the contractile ring, similar to control zygotes. This result suggests that the *myosin-II^{NMY-2}(ts)* mutation affects contractile ring constriction but not F-actin assembly, as expected (Figure 2B).

We then performed upshift experiments with *myosin-II^{NMY-2}(ts)* zygotes throughout cytokinesis. *Myosin-II^{NMY-2}(ts)* zygotes upshifted during cytokinesis up until the point of contractile ring closure failed to divide, whereas zygotes upshifted at any point after contractile ring closure completed cytokinesis (Figures 2C and 2D; Movie S1). Close examination of *myosin-II^{NMY-2}(ts)* zygotes upshifted 150 s after anaphase onset (well after the contractile ring had formed and constriction had begun) showed that the contractile ring immediately (≤10 s) paused for ~150 s, but then resumed constriction, albeit at a slower rate (Figure 2E). Slow ring constriction continued for ~300 s before the furrow regressed and cytokinesis failed. Thus, myosin-II^{NMY-2} activity is required for cytokinesis until just before contractile ring closure (Figure 7); however, myosin-II^{NMY-2} is not absolutely required for ring constriction itself.

Formin^{CYK-1} Actin-Nucleating Activity Is Only Required Early in Cytokinesis

We next examined the temporal requirement during cytokinesis for de novo linear F-actin assembly via the diaphanous-related formin^{CYK-1}, which nucleates and elongates linear F-actin, a component of the contractile ring. To this end, we identified a recessive fast-acting ts mutation in *formin^{CYK-1}*. We mapped the mutation to an L1015H substitution within the post region of the FH2 (formin homology) domain (Figure 3A; Table S1), required for lasso-post-mediated dimerization and processive F-actin polymerization (Otomo et al., 2005). This recessive mutation failed to complement two other *formin^{CYK-1}* alleles (Table S2). Finally, we found that upshifting *formin^{CYK-1}(ts)* zygotes during metaphase causes a full loss-of-function phenotype, with no furrow ingression and failure of cytokinesis (Figure S1).

To determine the biochemical effect of this point mutation, we characterized the ability of the ts mutant to polymerize F-actin in vitro and in vivo at restrictive temperature. We purified recombinant C-terminal fragments (FH1 and FH2 domains, amino acids 700–1,438) of wild-type formin^{CYK-1}(WT-FH1FH2C) and ts formin^{CYK-1}(ts-FH1FH2C) and compared their ability to stimulate F-actin assembly using an in vitro pyrene-actin assay, either alone or with the actin assembly cofactor profilin^{PFN-1}. Whereas formin^{CYK-1}(WT-FH1FH2C) stimulated actin assembly at low concentrations, formin^{CYK-1}(ts-FH1FH2C) showed no increase in assembly over the actin-only control in both the absence and presence of profilin^{PFN-1} (Figures 3B and 3C). To confirm this in vivo, we observed F-actin in *C. elegans* zygotes using a fluorescent F-actin reporter (Figure 3D). In control zygotes, a linear F-actin array localized to the cell cortex and was enriched at the cell equator, making up the contractile ring. *Formin^{CYK-1}(ts)* zygotes at 26°C ± 0.5°C lacked this array and F-actin appeared only in punctate structures (Figure 3D). These F-actin puncta appear to be independently nucleated by the Arp2/3 complex, as they were not seen following RNAi-mediated depletion of Arp2^{ARX-2} (Figure 3D). Together, these data suggest that this ts *formin^{CYK-1}* mutation disrupts the F-actin nucleation function for this protein.

Upshifts of *formin^{CYK-1}(ts)* zygotes at different time points throughout cytokinesis revealed that formin^{CYK-1}-mediated F-actin polymerization is only required early in cytokinesis (Figures 3E and 3F; Movie S2). Zygotes upshifted before initiation of constriction exhibited little or no furrowing, the characteristic full loss-of-function phenotype (Figure S1). Upshifts early during

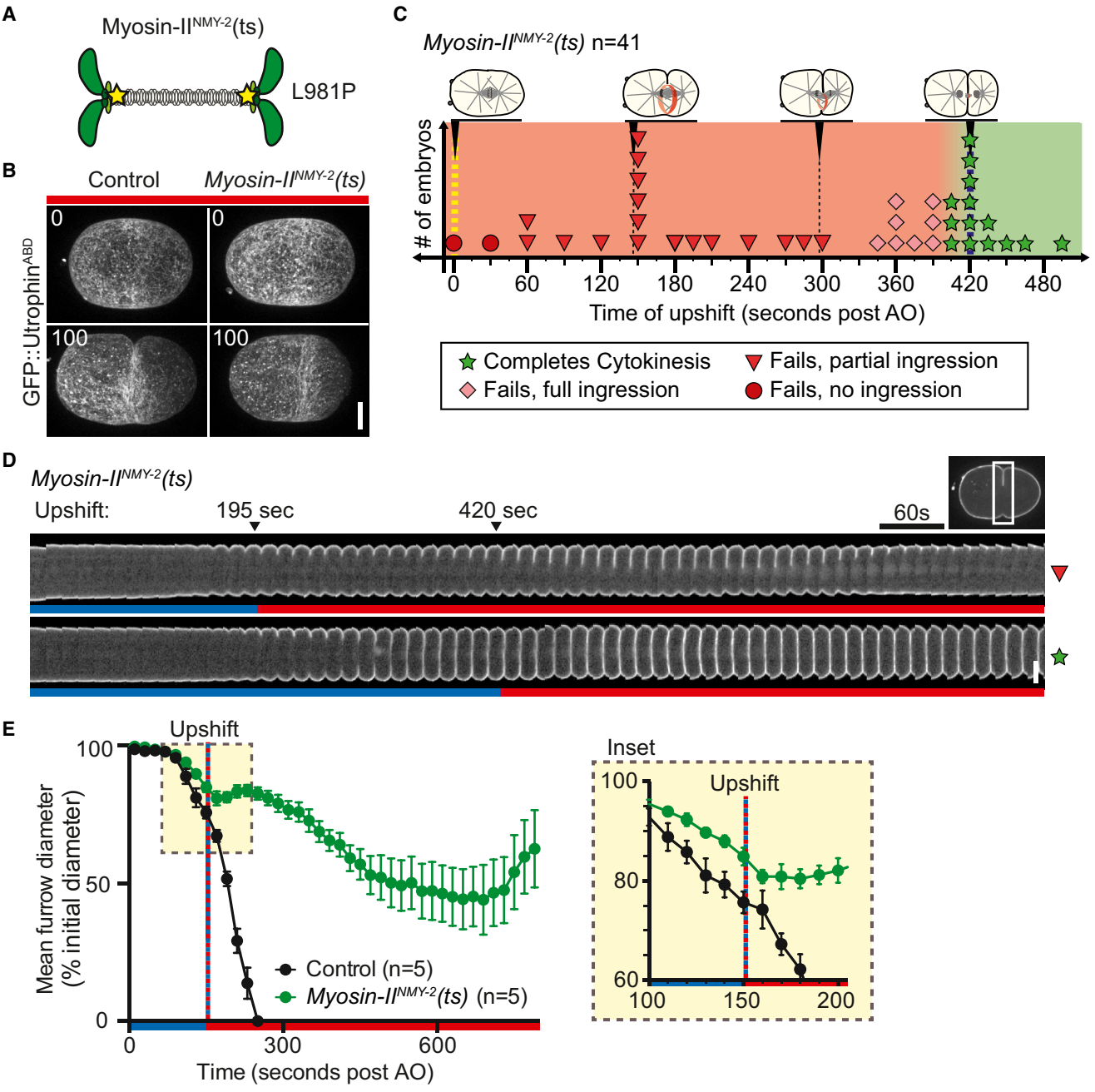

Figure 2. Myosin-II^{NMY-2} Activity Is Only Required during Contractile Ring Constriction

(A) Schematic of myosin-II^{NMY-2} oligomer. Yellow stars indicate the position of the ts mutation within the coiled-coil region proximal to the motor domain.

(B) GFP::Utrophin^{ABD}-labeled F-actin in control and *myosin-II^{NMY-2}(ts)* zygotes at 26°C ± 0.5°C.

(C) *Myosin-II^{NMY-2}(ts)* zygotes upshifted throughout cytokinesis. Each zygote is represented by a symbol plotted at the time of upshift relative to AO. The shape and color of each symbol indicate the success or failure of cytokinesis for that zygote. Color change of the graph background from coral to green indicates the end of the functional requirement for cytokinesis.

(D) Time-lapse montage of the division plane in *myosin-II^{NMY-2}(ts)* zygotes expressing GFP::PH (plasma membrane marker). Bar below montage represents temperature at each time point. Series begins one frame prior to AO.

(E) Mean furrow diameter over time in control and *myosin-II^{NMY-2}(ts)* mutant zygotes upshifted 150 s after AO. Inset highlights the immediate effect on ring constriction upon upshift. Time (s) is relative to AO. Measurements displayed as mean ± SEM. Blue, permissive; red, restrictive; AO, anaphase onset. Scale bar represents 10 μm.

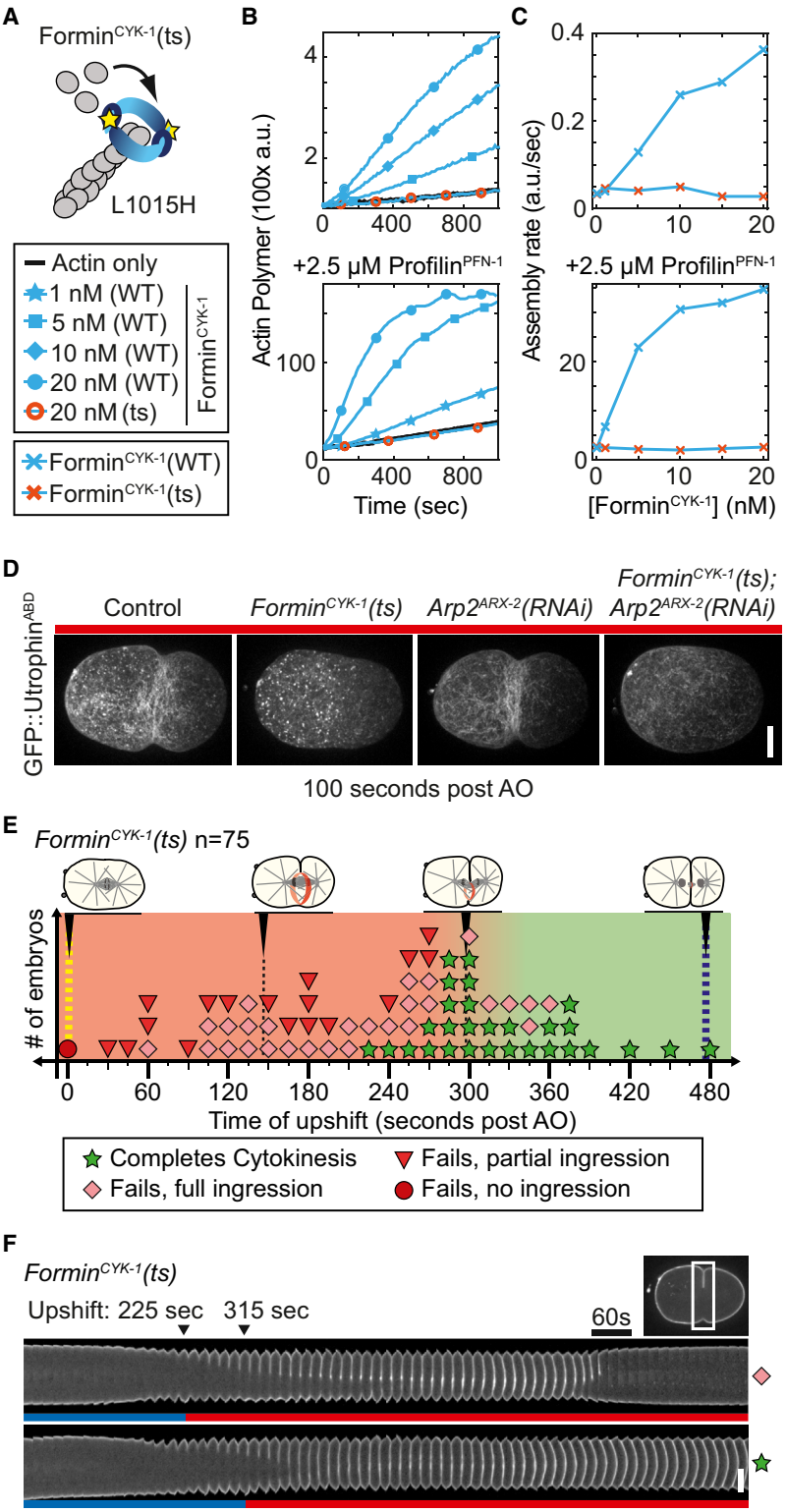

Figure 3. F-Actin Assembly by Formin^{CYK-1} Is Only Required Early in Cytokinesis

(A) Schematic of dimeric formin^{CYK-1} FH2 domains at the barbed end of an F-actin filament. Yellow stars indicate the position of the ts mutation within the post domain.

(B and C) In vitro polymerization of 20% pyrene-labeled Mg-ATP-actin monomers over time or (C) F-actin assembly rate with WT or ts formin^{CYK-1}(FH1FH2C) in the absence (left) or presence (right) of profilin^{PFN-1}.

(D) GFP::Utrophin^{ABD}-labeled F-actin in control, *formin^{CYK-1}(ts)*, *Arp2^{ARX-2}(RNAi)*, and *formin^{CYK-1}(ts); Arp2^{ARX-2}(RNAi)* zygotes at 26°C ± 0.5°C.

(E) *Formin^{CYK-1}(ts)* zygotes upshifted throughout cytokinesis. Each zygote is represented by a symbol plotted at the time of upshift relative to AO. The symbol colors, shapes, and graph background colors are defined as in Figure 2.

(F) Time-lapse montage of the division plane in *formin^{CYK-1}(ts)* zygotes expressing GFP::PH. Bar below montage represents temperature at each time point. Series begins one frame prior to AO. Time (s) is relative to AO. Blue, permissive; red, restrictive; AO, anaphase onset. Scale bar represents 10 μm.

constriction, just after cleavage furrow formation, also caused cytokinesis failure, although ring constriction often continued after the upshift (Figures 3E and 3F). In contrast, zygotes upshifted midway or late during constriction continued to constrict, maintained ring closure, and completed cytokinesis (Figures 3E and 3F). Therefore, formin^{CYK-1}-mediated de novo actin assembly is required early in cytokinesis but becomes dispensable midway through contractile ring constriction (Figure 7).

The Rac1 Pathway and Centralspindlin

Disrupting the Centralspindlin Complex after Contractile Ring Closure Blocks Cytokinesis

Centralspindlin is a heterotetrameric complex consisting of dimeric kinesin-6 microtubule motor MKLP1^{ZEN-4} and dimeric MgcRacGAP^{CYK-4}. We used two ts alleles (Figure 4A; Table S1) to block centralspindlin function: one with a D520N substitution in the centralspindlin-assembly domain of MKLP1^{ZEN-4} that disrupts the centralspindlin complex (Mishima et al., 2002), and the other with a T546I substitution in the GAP domain of MgcRacGAP^{CYK-4}, required for Rac1 inactivation (Canman et al., 2008). Both mutations cause full loss-of-function cytokinesis failure with only partial furrow ingression (Figure S1; Canman et al., 2008; Jantsch-Plunger et al., 2000; Mishima et al., 2002; Severson et al., 2000).

We first disrupted the centralspindlin complex during cytokinesis using the *MKLP1^{ZEN-4}(ts)* allele (Figures 4B and 4C; Movie S3). *MKLP1^{ZEN-4}(ts)* zygotes upshifted during contractile ring constriction always failed in cytokinesis. Zygotes upshifted shortly after contractile ring closure showed a mixed phenotype, with furrow regression in some zygotes and cytokinesis completion in others. Zygotes upshifted more than 120 s after contractile ring closure consistently completed cytokinesis. To determine the effect of upshifts on centralspindlin integrity, we generated *MKLP1^{ZEN-4}(ts)*

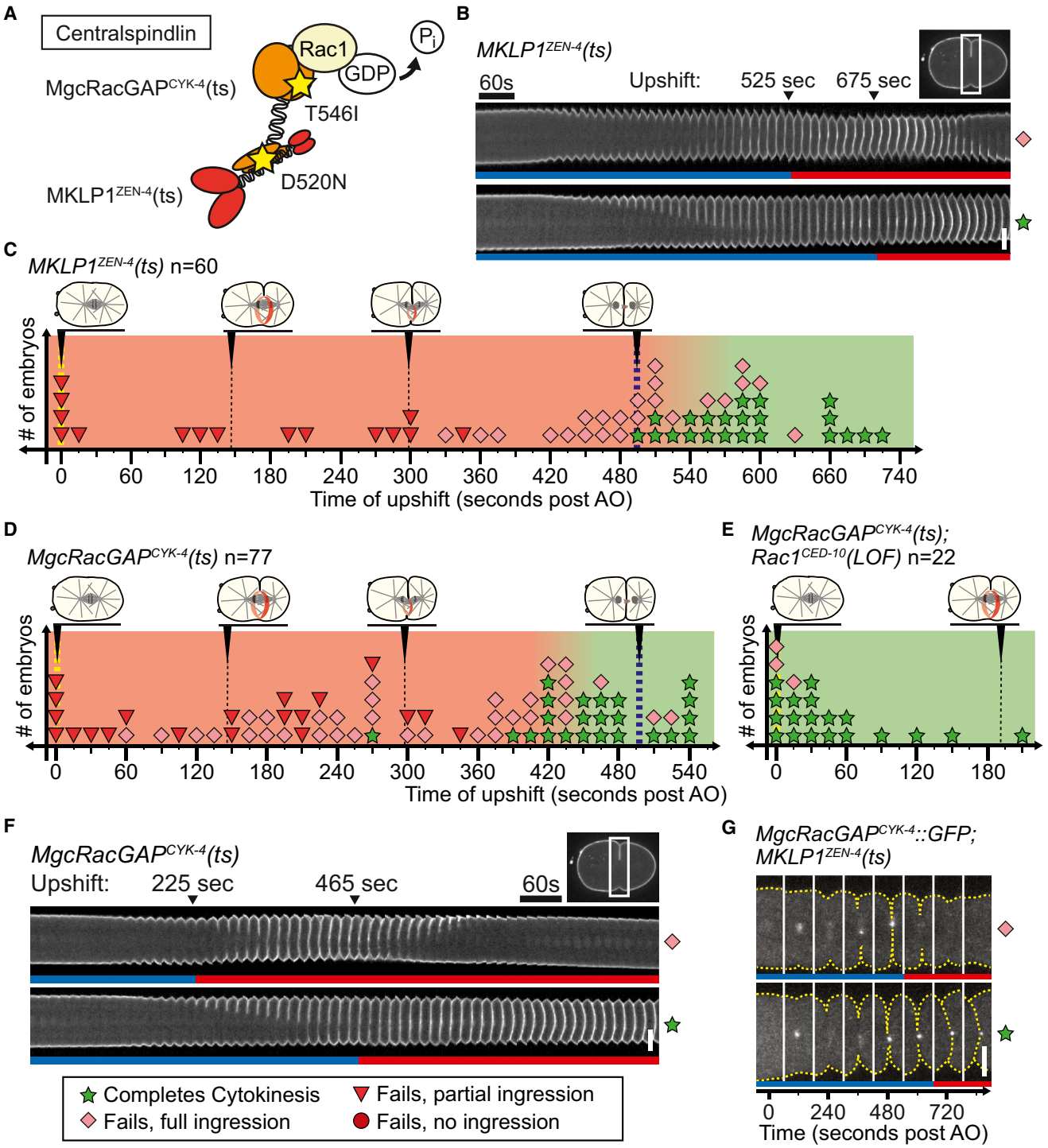

Figure 4. Different Centralspindlin Functions Are Required at Different Times during Cytokinesis

(A–F) Schematic of tetrameric centralspindlin, composed of dimeric MKLP1^{ZEN-4} and dimeric MgcRacGAP^{CYK-4}. Stars indicate the position of the ts mutations within the GAP domain of MgcRacGAP^{CYK-4} and centralspindlin assembly domain of MKLP1^{ZEN-4}. (C) *MKLP1^{ZEN-4}(ts)*, (D) *MgcRacGAP^{CYK-4}(ts)*, and (E) *MgcRacGAP^{CYK-4}(ts)*; Rac1^{CED-10}(LOF) double mutant zygotes upshifted throughout cytokinesis. Each zygote is represented by a symbol plotted at the time of upshift relative to AO. The symbol colors, shapes, and graph background colors are defined as in Figure 2. (B and F) Time-lapse montage of the division plane in (B) *MKLP1^{ZEN-4}(ts)* and (F) *MgcRacGAP^{CYK-4}(ts)* mutant zygotes expressing a GFP::PH (plasma membrane marker). Bar below montage represents temperature at each time point. Series begins one frame prior to AO.

(G) Time-lapse montage of the division plane in *MKLP1^{ZEN-4}(ts)* zygotes expressing MgcRacGAP^{CYK-4}::GFP (see also Figure S2). Time (s) is relative to AO. Blue, permissive; red, restrictive; AO, anaphase onset. Scale bar represents 10 μm.

mutants expressing a GFP-tagged MgcRacGAP^{CYK-4} (Verbrugghe and White, 2004). Zygotes upshifted less than 500 s after anaphase onset failed cytokinesis, and midbody-targeted MgcRacGAP^{CYK-4}::GFP was lost. In contrast, zygotes upshifted later (>600 s after anaphase) divided successfully, and MgcRacGAP^{CYK-4}::GFP remained at the midbody (Figures 4G and S2). Thus, the role of MKLP1^{ZEN-4} in maintaining MgcRacGAP^{CYK-4} at the division plane is required from anaphase onset, throughout cytokinesis, and for a short time following ring closure (Figure 7).

MgcRacGAP^{CYK-4} GAP Activity Is Required from Anaphase Onset until Late in Contractile Ring Constriction

To determine the functional time window for GAP activity of centralspindlin, we used a second ts allele containing a point mutation in a conserved functional residue within the GAP domain (Figure 4A; Table S1) of MgcRacGAP^{CYK-4} (Canman et al., 2008). This allele is a centralspindlin separation-of-function mutant that specifically affects the MgcRacGAP^{CYK-4} GAP domain but does not disrupt central spindle assembly or MKLP1^{ZEN-4} localization (Canman et al., 2008). Consistent with previous reports (Canman et al., 2008; Loria et al., 2012), *MgcRacGAP^{CYK-4}(ts)* zygotes upshifted prior to anaphase onset failed to divide with only partial furrow ingression (Figure S1). To determine the temporal requirement of centralspindlin GAP activity, we upshifted *MgcRacGAP^{CYK-4}(ts)* zygotes throughout cytokinesis (Figures 4D and 4F; Movie S4). Zygotes upshifted shortly after anaphase onset and before cleavage furrow formation formed a contractile ring that only partially constricted before failing in cytokinesis. Zygotes upshifted at intermediate times during contractile ring constriction underwent full ring constriction, but eventually cytokinesis failed. However, zygotes upshifted less than 60 s prior to closure (~420 s after AO) were often able to maintain separation of the daughter cells. These results suggest that, in contrast to MKLP1^{ZEN-4}-dependent centralspindlin integrity, MgcRacGAP^{CYK-4} GAP activity is not required during the very late stages of cytokinesis (Figure 7).

It was previously found that the cytokinesis defects in *MgcRacGAP^{CYK-4}(ts)* zygotes could be suppressed by inactivation of the target GTPase Rac1^{CED-10} (Canman et al., 2008; Loria et al., 2012). We sought to determine whether inhibition of Rac1^{CED-10} in *C. elegans MgcRacGAP^{CYK-4}(ts)* mutant zygotes was more effective at any specific stage in cytokinesis. We generated an *MgcRacGAP^{CYK-4}(ts); Rac1^{CED-10}(LOF)* double mutant strain, in which Rac1^{CED-10} is locked in the "off" GDP-bound conformation by a G60R substitution (Reddien and Horvitz, 2000). Almost no division failure was observed when these zygotes were upshifted throughout cytokinesis (Figure 4E). Together, these data suggest that GAP activity of MgcRacGAP^{CYK-4} is required to inactivate Rac throughout cytokinesis but this becomes dispensable at contractile ring closure (Figure 7).

The Chromosomal Passenger Complex

The CPC Is Required Early in Mitosis for Efficient Cell Division but Is Dispensable during Cytokinesis

We systematically inactivated CPC function from early prophase onward using both a P265L Aurora-B^{AIR-2} kinase-defective ts allele used previously (Severson et al., 2000) and a ts allele with an A551T substitution near the "IN box" of INCENP^{ICP-1}, a domain required for full kinase activity (Figure 6A; Tables S1 and S2; Bishop and Schumacher, 2002). *Aurora-B^{AIR-2}(ts)* zygotes upshifted early in mitosis (during prophase at pronuclear meeting) exhibited the full loss-of-function CPC phenotype: massive chromosome segregation errors, only partial contractile ring constriction, and cytokinesis failure (Figure S1). Because Aurora-B^{AIR-2} kinase has mitotic, as well as cytokinetic roles, we upshifted *Aurora-B^{AIR-2}(ts)* zygotes at different time points throughout mitosis and cytokinesis. Zygotes upshifted before nuclear envelope breakdown (NEBD) failed in both chromosome segregation and cytokinesis. Surprisingly, zygotes upshifted during late prometaphase or beyond, were able to complete cytokinesis (Figures 5B and 5C; Movie S5). This result suggests that full Aurora-B^{AIR-2} activity is required at an early stage of mitosis but not later in mitosis for successful completion of contractile ring constriction during cytokinesis (Figure 7).

To confirm that the window of CPC activity required for cytokinesis occurred well before anaphase onset, we upshifted *Aurora-B^{AIR-2}(ts)* zygotes for brief (~180 s) windows throughout early mitosis, then downshifted them to the permissive temperature to restore protein function. Again, we found that zygotes upshifted for ~180 s just prior to NEBD through early prometaphase failed in cytokinesis, even when activity was restored by returning the zygotes to permissive temperature prior to anaphase onset (Figure 5D). *Aurora-B^{AIR-2}(ts)* zygotes briefly upshifted either before or after this window were able to undergo cytokinesis (Figure 5D). This result highlights the fast-acting nature of the *Aurora-B^{AIR-2}(ts)* mutation, and further demonstrates that the window of cytokinetic requirement for Aurora-B^{AIR-2} activity actually occurs well before anaphase onset (Figure 7).

To confirm the temporal requirement of CPC function, we identified a recessive fast-acting ts allele of *INCENP^{ICP-1}* with a fully penetrant CPC loss-of-function phenotype at restrictive temperatures (Figure S1; Table S2). This mutation lies within the "IN box" (Figure 6A; Table S1), a region of INCENP^{ICP-1} known to be important for Aurora-B^{AIR-2} binding and kinase activation (Bishop and Schumacher, 2002; Honda et al., 2003; Xu et al., 2009). To determine if activation of Aurora-B^{AIR-2} is disrupted by the ts mutation in INCENP^{ICP-1}, we performed in vitro kinase assays (Figure 6B). We copurified recombinant Aurora-B^{AIR-2} with either INCENP^{ICP-1}(WT-IN box) or INCENP^{ICP-1}(ts-IN box) proteins. The amount of INCENP^{ICP-1}(ts-IN box) pulled down was slightly reduced compared to INCENP^{ICP-1}(WT-IN box), indicating the ts mutation disrupts complex formation (Figure 6B). Furthermore, measurement of the kinase activity of these two complexes determined that both phosphorylation of INCENP^{ICP-1} and Aurora-B^{AIR-2} auto-phosphorylation is further reduced in the complex containing the ts mutation (Figure 6B). This indicates that the *INCENP^{ICP-1}(ts)* mutation causes a disruption in the activation feedback loop required for Aurora-B^{AIR-2} kinase activity.

We then performed upshift experiments on *INCENP^{ICP-1}(ts)* zygotes (Figures 6C and 6D; Movie S6). Zygotes upshifted before NEBD failed in both chromosome segregation and cytokinesis, whereas those upshifted late in prometaphase were able to divide successfully. Furthermore, similar to the results with *Aurora-B^{AIR-2}(ts)*, we found that upshifting *INCENP^{ICP-1}(ts)* zygotes early in mitosis for brief periods (~180 s) also inhibited cytokinesis, confirming rapid loss of protein function (Figure 6F).

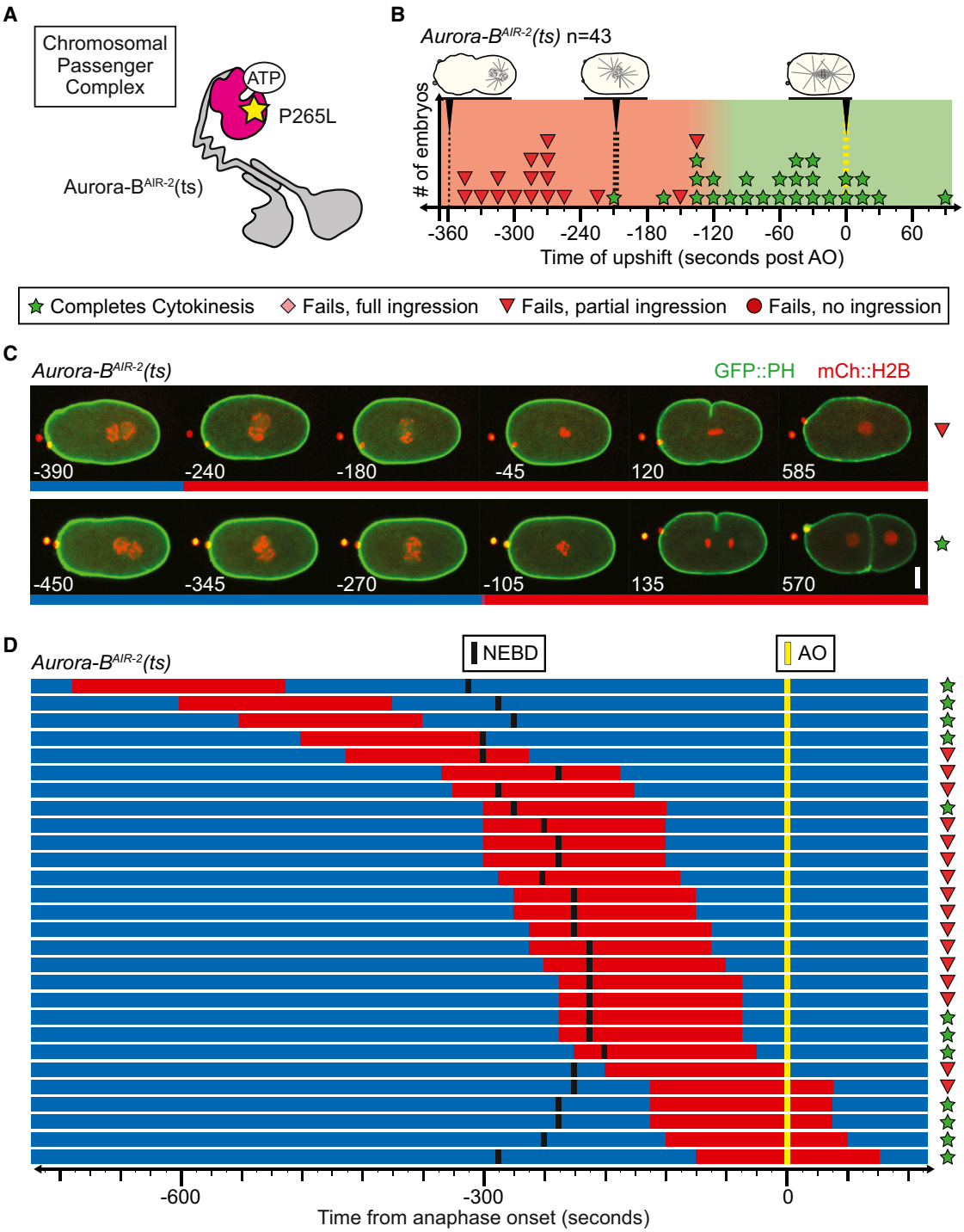

Figure 5. Aurora-B^{AIR-2} Kinase Activity Is Not Required during Cytokinesis

(A) Schematic of the CPC. Aurora-B^{AIR-2} kinase is highlighted in pink. Yellow star indicates the position of the ts mutation within the kinase domain.

(B) *Aurora-B^{AIR-2}(ts)* zygotes upshifted throughout mitosis. Each zygote is represented by a symbol plotted at the time of upshift relative to AO. The symbol colors, shapes, and graph background colors are defined as in Figure 2.

(C) Time-lapse montage of *Aurora-B^{AIR-2}(ts)* zygotes expressing GFP::PH to label the plasma membrane (green) and mCherry::H2B to label the chromosomes (red). Bar below montage represents temperature at each time point.

(D) *Aurora-B^{AIR-2}(ts)* zygotes upshifted only for brief periods (~180 s) early in mitosis. Time (s) is relative to AO. Blue, permissive; red, restrictive; AO, anaphase onset; NEBD, nuclear envelope breakdown. Scale bar represents 10 μm.

These results using the *INCENP^{ICP-1}(ts)* allele thus corroborates that, at least in *C. elegans* zygotes, full CPC activity is required early in mitosis, but is not absolutely required during cytokinesis (Figure 7).

To determine if inactive CPC is still able to "passenge" to the central spindle, we crossed the *INCENP^{ICP-1}(ts)* allele into a strain expressing GFP::Aurora-B^{AIR-2}. Zygotes upshifted during metaphase completed cytokinesis and showed GFP::Aurora-B^{AIR-2} passenging from the chromosomes to the central spindle during anaphase (Figure 6E). Zygotes upshifted in or before early prometaphase failed massively in both chromosome segregation and cytokinesis, and GFP::Aurora-B^{AIR-2} briefly remained on the chromosomes during anaphase. Normal localization is likely precluded due to the lack of central spindle formation caused by severe chromosome segregation defects. Although full Aurora-B^{AIR-2} activity is not required after metaphase, it is still possible that successful CPC passenging to central spindle microtubules is required for cytokinesis.

Although cytokinesis could still complete in the absence of Aurora-B^{AIR-2} kinase activity during metaphase and anaphase, we wanted to determine if this inactivation affected central spindle microtubules, as was recently reported (Douglas et al., 2010; Nunes Bastos et al., 2013; Uehara et al., 2013). As we found that inactive CPC is still able to "passenge" to the central spindle (Figure 6E), we used the GFP::Aurora-B^{AIR-2} marker to observe central spindle microtubules. We upshifted control and *INCENP^{ICP-1}(ts)* zygotes at metaphase alignment and imaged GFP::Aurora-B^{AIR-2} after anaphase onset (Figure S3). At 240 s after anaphase onset in control zygotes, GFP::Aurora-B^{AIR-2} had passenged from the chromosomes to central spindle microtubules, appearing as a punctate structure at the center of the midbody. However, in *INCENP^{ICP-1}(ts)* zygotes, the midbody was elongated, with GFP::Aurora-B^{AIR-2} localizing to a region twice as long as control cells (Figure S3), suggesting misregulation of the central spindle and midbody structure. Thus, the CPC is required to form a compact midbody late in cytokinesis; however, this function is not essential for successful cell division.

DISCUSSION

We developed a device, the Therminator, to rapidly alter sample temperature and study the temporal regulation of cytokinesis in combination with fast-acting ts cytokinesis-defective mutants. We assessed the molecular temporal profiles for three major signaling pathways thought to control cytokinesis (Figure 1A): (1) The RhoA pathway, which promotes actomyosin assembly and activation; (2) The Rac1 pathway, which is inhibitory to cytokinesis and must be held inactive for successful division; and (3) the CPC pathway, which blocks cytokinesis upon functional disruption via an unknown molecular mechanism. Our results show that each of these pathways function in distinct temporal intervals indicating the molecular control of cytokinesis is complex and highly regulated throughout the stages of cell division.

Myosin-II^{NMY-2}

We started with a fast-acting ts mutant of myosin-II^{NMY-2} that had previously been analyzed by a similar method. Liu et al. (2010) found that myosin-II^{NMY-2} was required throughout contractile ring constriction and for 180 s after ring closure to prevent late cytokinesis failure and binucleation. In agreement with Liu et al. (2010), we found myosin-II^{NMY-2} activity was required throughout constriction of the contractile ring for the successful completion of cytokinesis. However, in contrast with this previous study, our data suggest that myosin-II^{NMY-2} activity is only required until the time of contractile ring closure. In the previous study, temperature upshifts relied on passive heat transfer and required about 70 s (or approximately one-fifth of cytokinesis) to achieve full protein inactivation. Further, the kinetics of cytokinesis were monitored by differential interference contrast rather than four-dimensional spinning disc confocal microscopy, which is less precise when used to determine the time of anaphase onset and contractile ring closure. Thus, our myosin-II^{NMY-2} results highlight the importance of rapid temperature upshifts and high-resolution in vivo analysis to precisely determine the functional window for proteins during cell division.

We also confirmed the finding that upshifts of *myosin-II^{NMY-2}(ts)* zygotes did not completely abolish further constriction of the contractile ring once the ring had already initiated constriction (Liu et al., 2010). This finding, supporting a myosin-II^{NMY-2}-independent constriction mechanism, is not the first to challenge classical paradigms of ring constriction driven solely by the sliding of myosin-II^{NMY-2} motors along F-actin. In budding yeast, myosin-II lacking the motor domain is sufficient to support cytokinesis (Fang et al., 2010; Mendes Pinto et al., 2012), albeit with significantly reduced ring constriction rates (Mendes Pinto et al., 2012). Recent work in mammalian cultured cells has similarly shown that the motor activity of myosin-II is not required for cytokinesis. Ma and colleagues found that in the absence of myosin-II-based motility, cytokinesis continued as long as myosin-II retained the ability to crosslink actin filaments and maintain tension (Ma et al., 2012). Similarly, actin crosslinking (coupled to F-actin depolymerization) has also been found to provide contractile force during cytokinesis in some systems (Reichl et al., 2008; Zumdieck et al., 2007), and myosin-II independent closure of a contractile ring was found in studies of cell wound healing (Burkel et al., 2012). Curiously, Burkel et al. (2012) found that the rate of ring closure around cellular wounds was significantly reduced following myosin-II inhibition, as also observed here. Based on the myosin-II independence and other findings, it was proposed that the closure resulted from a ring-like gradient of RhoA activation and inactivation (a "signal treadmill") coupled to differential actin assembly and disassembly (Burkel et al., 2012). A similar mechanism may be used during cytokinesis, although this possibility has yet to be tested.

Formin^{CYK-1}-Nucleated F-Actin

F-actin assembly and filament turnover have been proposed to function throughout cytokinesis for effective contractile ring assembly and constriction (Murthy and Wadsworth, 2005; Pelham and Chang, 2002). However, more recently, it was shown that a chemical inhibitor of F-actin assembly, Latrunculin A, did not block cytokinesis when applied to cells after the contractile ring had formed, suggesting that de novo F-actin assembly is not required for contractile ring constriction (Carvalho et al., 2009; Proctor et al., 2012). Similarly, blocking actin polymerization did not inhibit contractile ring constriction in an in vitro yeast cytokinesis model (Mishra et al., 2013). This fits with electron microscopy studies in echinoderm embryos and fission yeast

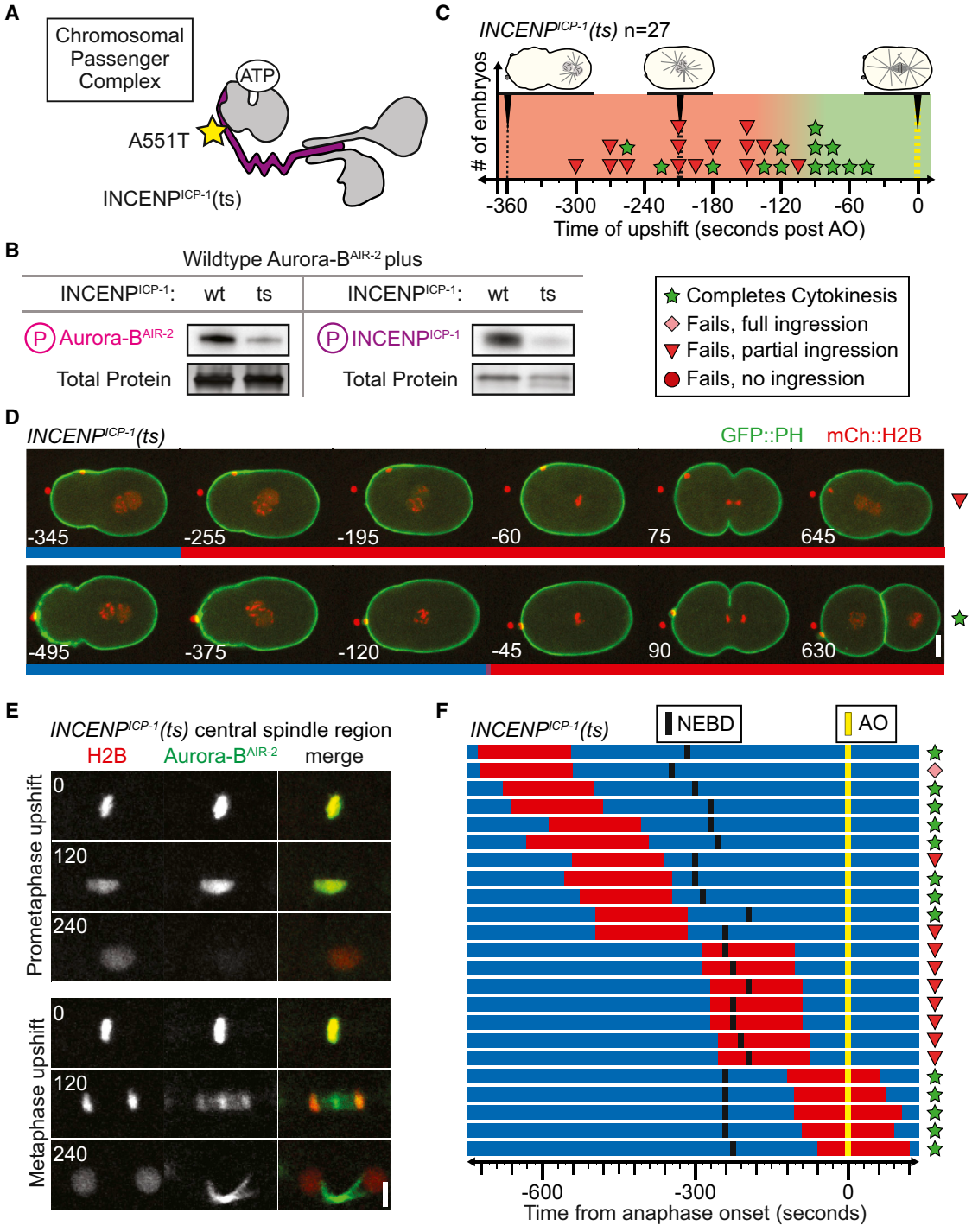

Figure 6. Abrogating CPC Function after Prometaphase Disrupts the Central Spindle but Does Not Prohibit Cytokinesis

(A) Schematic of the CPC, INCENP^{ICP-1} is highlighted in purple. Yellow star indicates the position of the ts mutation within the IN box.

(B) In vitro kinase activity of recombinant Aurora-B^{AIR-2} in the presence of WT or ts INCENP^{ICP-1} C-terminal IN box. Phosphorylation of Aurora-B^{AIR-2} (left) and INCENP^{ICP-1} (right) was reduced in the presence of ts INCENP^{ICP-1} IN box compared with WT INCENP^{ICP-1} IN box. Total protein amounts are comparable between WT and ts INCENP^{ICP-1} complexes as depicted with by silver stain.

(C) *INCENP^{ICP-1}(ts)* zygotes upshifted throughout mitosis. Each zygote is represented by a symbol plotted at the time of upshift relative to AO. The symbol colors, shapes, and graph background colors are defined as in Figure 2.

(legend continued on next page)

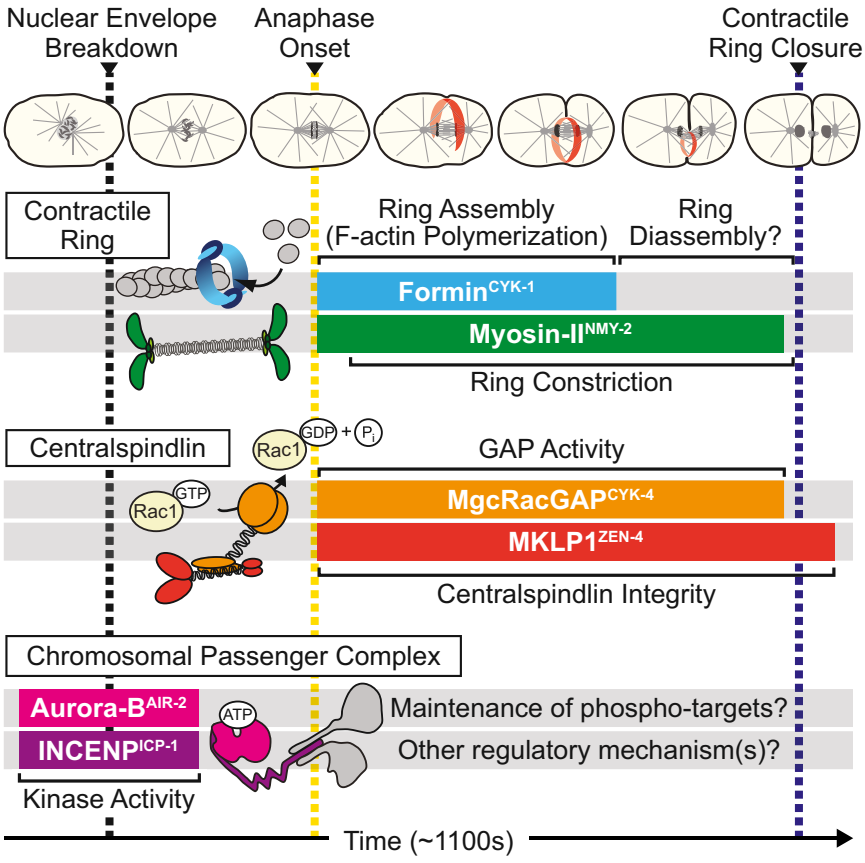

Figure 7. Summary of the Temporal Requirement of Cytokinetic Protein Functions for Cytokinesis

Temporal requirement for the protein functions analyzed in this study displayed relative to cell division stages. The colored bar represents the period during which disruption of protein function leads to cytokinesis failure. Time is not drawn to scale.

showing that the volume of the contractile ring decreases relative to its diameter during late constriction, suggesting a balance of F-actin dynamics favoring disassembly (Kamasaki et al., 2007; Schroeder, 1972). Our data support a model in which de novo F-actin polymerization by formin^{CYK-1} is not required for cytokinesis once the contractile ring has been assembled and initiates constriction.

Centralspindlin: Kinesin-6 MKLP1^{ZEN-4} and MgcRacGAP^{CYK-4}

To parse out the different temporal requirements of two centralspindlin functions, we used ts mutants in the kinesin-6 MKLP1^{ZEN-4} and the Rac GAP MgcRacGAP^{CYK-4}. The *MKLP1^{ZEN-4}(ts)* mutation used here disrupts binding between MKLP1^{ZEN-4} and MgcRacGAP^{CYK-4}, which is required for most centralspindlin functions (Canman et al., 2008; Pavicic-Kaltenbrunner et al., 2007; Severson et al., 2000). This *MKLP1^{ZEN-4}(ts)* allele was previously found to disrupt cytokinesis when zygotes were upshifted very late (~300 s) after contractile ring closure using passive heat transfer (Severson et al., 2000). Our data confirmed that MKLP1^{ZEN-4} is required throughout contractile ring assembly and constriction until very late in cytokinesis, including a short period after ring closure. However, with the improved resolution of our temporal analysis, we found *MKLP1^{ZEN-4}(ts)* mutant zygotes maintained separation when the upshift occurred > 150 s after closure of the ring. In contrast to this extended requirement for centralspindlin integrity, MgcRacGAP^{CYK-4} GAP activity was only required until late in cytokinesis, usually just before the contractile ring closed.

The requirement for centralspindlin integrity after contractile ring closure suggests that the complex plays an important structural role very late in cytokinesis, perhaps by regulating microtubules of the midbody, a tightly focused region containing antiparallel microtubules and hundreds of other proteins (Hu et al., 2012; Skop et al., 2004). The midbody is thought to play an important role in abscission. However, in early *C. elegans* zygotes, abscission occurs well after ring closure (>800 s) and is independent of midbody microtubules. Further, in the worm zygote, abscission failure does not lead to regression of the contractile ring (Green et al., 2013). We do not know if centralspindlin, or any of the proteins studied here, are involved in this late step.

Despite the loss of centralspindlin integrity seen in earlier upshifts, we found that MgcRacGAP^{CYK-4}::GFP is maintained at the midbody in *MKLP1^{ZEN-4}(ts)* mutant zygotes upshifted ~120 s after contractile ring closure. This could be due to centralspindlin clustering (Hutterer et al., 2009) preventing the ts mutation from disrupting the complex, or due to association of MgcRacGAP^{CYK-4} with another midbody protein. Alternatively, it could be due to autonomous MgcRacGAP^{CYK-4} localization via the C1 domain, which directly binds to the cell membrane late in cytokinesis (Lekomtsev et al., 2012). Regardless, our data suggest a transition point following contractile ring closure, after which MgcRacGAP^{CYK-4} localization at the midbody is likely independent of binding to MKLP1^{ZEN-4}.

(D) Time-lapse montage of *INCENP^{ICP-1}(ts)* zygotes expressing GFP::PH to label the plasma membrane (green) and mCherry::H2B to label the chromosomes (red). Bar below montage represents temperature at each time point. Scale bar represents 10 μm.
(E) Time-lapse images of the mitotic spindle region in *INCENP^{ICP-1}(ts)* zygotes expressing mCherry::H2B (red) and GFP::Aurora-B^{AIR-2} (green), upshifted in prometaphase (top) or metaphase (bottom). Scale bar represents 5 μm.
(F) *INCENP^{ICP-1}(ts)* zygotes upshifted for brief periods (~180 s) early in mitosis. Time (s) is relative to AO. Blue, permissive; red, restrictive; AO, anaphase onset; NEBD, nuclear envelope breakdown.

The exact role of the MgcRacGAP^{CYK-4} GAP domain has been subject to some controversy. However, in *C. elegans* (Canman et al., 2008), *Drosophila* (D'Avino et al., 2004), and mammalian culture cells (Bastos et al., 2012), GAP domain mutants can be suppressed by inhibition of Rac1 or its effectors, suggesting it downregulates this small GTPase. Consistent with this, we found that inhibition of Rac-1^{CED-10} activity can suppress the cytokinesis failure caused by inactivation of MgcRacGAP^{CYK-4} GAP activity throughout cytokinesis. This further supports a model in which the GAP domain of MgcRacGAP^{CYK-4} inhibits Rac1^{CED-10} activity throughout contractile ring constriction but not beyond ring closure. Perhaps active Rac1^{CED-10} is not inhibitory to the very final stage of cytokinesis, or the GAP activity of centralspindlin is not functioning late in division.

The Chromosomal Passenger Complex

Chronic inhibition of the CPC by depletion or other approaches causes massive chromosome segregation defects and cytokinesis failure (Carmena et al., 2012; Douglas et al., 2010; Severson et al., 2000). However, previous temporal analysis using the ts allele of *Aurora-B^{AIR-2}* and an upshift assay showed that kinase activity is not required during cytokinesis (Severson et al., 2000), a result that has been largely overlooked. Using two conditional ts CPC alleles, we indeed found that the full loss-of-function phenotype was replicated only when zygotes were upshifted prior to NEBD. In contrast, if kinase inactivation occurred late in prometaphase or beyond, chromosome segregation proceeded successfully and cytokinesis completed. We could also recapitulate cytokinesis failure in ts CPC mutant zygotes briefly upshifted for a window early in mitosis, even when the zygotes were returned to permissive temperature before anaphase onset. These results conflict with a simple model in which Aurora-B^{AIR-2} passenges from chromosomes to the central spindle at anaphase where its kinase activity is essential for phosphorylation of protein targets that directly promote contractile ring constriction. Our data instead suggest that in *C. elegans* zygotes, Aurora-B^{AIR-2} substrates that are required for full ring constriction during cytokinesis are phosphorylated during prophase or early prometaphase, when the CPC is still on the chromosomes.

While we cannot completely exclude the possibility that there is residual Aurora-B^{AIR-2} kinase activity at the restrictive temperature, several lines of evidence suggest that this residual kinase activity is not responsible for facilitating cytokinesis in ts zygotes held at the restrictive temperature. First, upshift of the ts mutant prior to NEBD produces an identical chromosomal phenotype seen following depletion of the CPC by RNAi (Kaitna et al., 2000). Second, previous work in cultured DT40 cells showed that higher levels of Aurora-B kinase activity are required for cytokinesis than chromosome segregation in early mitosis (Xu et al., 2010). Third, the same *Aurora-B^{AIR-2}(ts)* mutant allele used in our studies has been shown by immunofluorescence to completely eliminate the Aurora-B^{AIR-2}-dependent phosphorylation of metaphase HistoneH3-S10 in vivo when maintained at 25°C (Collette et al., 2011). Furthermore, this mutation has been shown to completely block kinase activity in vitro (Bishop and Schumacher, 2002). Finally, previously identified genetic suppressors of the same *Aurora-B^{AIR-2}(ts)* allele were only able to suppress the mutant phenotype at intermediate temperatures (20-22°C) but not at the completely restrictive temperature (de Carvalho et al., 2008; Heallen et al., 2008), suggesting that kinase activity is too substantially reduced at 26°C (the restrictive temperature used here) to be rescued. Because we see the same loss-of-function phenotype and temporal requirement for both *Aurora-B^{AIR-2}(ts)* and *INCENP^{ICP-1}(ts)* zygotes, we propose that kinase activity is dramatically reduced in both ts mutants and that kinase activity is not required at late stages of mitosis for successful completion of cytokinesis. Consistent with this, a brief window of upshift early in mitosis followed by return to permissive temperature does not rescue cytokinesis failure in ts CPC mutant zygotes. Thus, we propose that Aurora-B^{AIR-2} kinase activity after anaphase onset, whether full or residual, is not sufficient to facilitate successful contractile ring constriction during cytokinesis when functionally blocked early in mitosis. Taken together, these data suggest that, at least in *C. elegans* zygotes, the major contribution of the CPC to cytokinesis occurs very early in mitosis.

Our results demonstrate the importance of high-resolution temporal analysis in generating new paradigms for protein function. For example, these data raise interesting questions about Aurora-B^{AIR-2} phosphorylation targets in prometaphase. Are these novel or previously identified targets of Aurora-B^{AIR-2}? Are these phosphorylation events stably maintained throughout cytokinesis in the absence of Aurora-B^{AIR-2} kinase activity or do these phosphorylation events trigger another signaling cascade that mediates cytokinesis? Alternatively, do these phosphorylation events lead to a structural interaction that is later required for cytokinesis? Due to the incompatibility of the Therminator with conventional immunofluorescence of worm embryos, determination of Aurora-B^{AIR-2} activity in *C. elegans* will require the development of Aurora-B^{AIR-2}-specific biosensors for use in vivo.

By combining rapid temperature upshifts with conditionally inactive ts mutants, we were able to make direct in vivo functional comparisons between the temporal requirements of different proteins during cell division within the same model system, producing a functional molecular timeline for cytokinesis. Together, our data illustrate that individual protein functions are uniquely regulated along the cell division timeline, resulting in proteins with very similar localization and loss-of-function phenotypes being required for cytokinesis at overlapping but distinct times. Here we have focused our studies on the temporal regulation of cytokinesis; however, the same experimental approach could be used in studies on any biological process in model systems for which fast-acting ts mutations are available. The next important frontier will be to develop conditional approaches to probe the spatiotemporal regulation of cell division and determine the subcellular active pool(s) of proteins essential for cytokinesis.

EXPERIMENTAL PROCEDURES

Strain Maintenance

Worm strains were maintained at 16.0°C ± 0.5°C on standard NGM plates seeded with OP50 (Brenner, 1974).

Mutant Cloning and Rescue Experiments

Formin^{CYK-1}(ts) [*cyk-1(or596ts)*] and *INCENP^{ICP-1}(ts)* [*icp-1(or663ts)*] were identified in an ENU mutagenesis screen for ts cytokinesis-defective mutations

(Table S2; Encalada et al., 2000; O'Connell et al., 1998). Both alleles were mapped using 3-factor visible marker mapping as described (Brenner, 1974) (see Supplemental Experimental Procedures). *icp-1(or663ts)* and *cyk-1(or596ts)* were backcrossed 6× against N2 males prior to phenotypic analysis.

Temperature Control for Imaging

Live imaging was performed in a temperature-controlled room. Microscope temperature was continuously monitored using three digital thermometers attached directly to the objective lens. For Therminator experiments, the room was equilibrated to an intermediate temperature, depending on the ts mutant. See Supplemental Experimental Procedures for more details.

Imaging and Quantitative Analysis

Gravid worms were dissected in M9 buffer (Brenner, 1974) and mounted as previously described (Gönczy et al., 1999). Embryos were filmed using a Yokagawa CSU-10 spinning disc confocal with Borealis (Spectral Applied Research) on a Nikon Ti inverted microscope with either a 20× 0.75 N.A. dry, a 40× 0.95 N.A. dry, or a 60× 1.4 N.A. oil-immersion PlanApochromat objective with 2 × 2 binning on a Hamamatsu Orca ER camera. Z-sectioning was done with a Piezo-driven motorized stage (Applied Scientific Instrumentation) and focus was maintained using Perfect Focus (Nikon) prior to each Z-section acquisition. An acousto-optic tunable filter was used to select the excitation light of two 100 mW lasers for excitation at 491 and 561nm for eGFP and mCherry, respectively (Spectral Applied Research), and a filter-wheel was used for emission wavelength selection (Sutter Instruments). The system was controlled by MetaMorph software (Molecular Devices). See Supplemental Experimental Procedures for more details.

Rapid Temperature Shifts

Rapid temperature shifts were performed using a custom-built fluidic system called the Therminator (Figure 1B, Bioptechs) with one water/isopropanol bath at permissive temperature (16°C ± 0.5°C) and a second bath at the restrictive temperature (26°C ± 0.5°C). A switch mechanism determines which water bath supplies liquid for the chamber above the specimen. Forced heat convection from the flow chamber to the glass barrier directly above the specimen chamber rapidly shifts the sample temperature.

In Vitro Pyrene F-Actin Polymerization Assays

Formin^{CYK-1} WT- and ts-FH1FH2C domains and profilin^{PFN-1} were purified from *Escherichia coli*. Ca-ATP actin was purified from rabbit skeletal muscle (Spudich and Watt, 1971), and gel-filtered actin was labeled on Cys-374 with pyrene (Kuhn and Pollard, 2005; Neidt et al., 2008). Spontaneous actin assembly was measured from the fluorescence of a trace of pyrene-actin at 25°C. See Supplemental Experimental Procedures for more details.

Feeding RNAi

cDNA for *arx-2* was cloned into the multiple cloning site of the L4440 vector and then transformed into HT115 *E. coli* using $CaCl_2$ transformation (Timmons et al., 2001). L1 worms were plated on RNAi plates and incubated at 16°C ± 0.5°C for 72 hr prior to filming. RNAi efficiency was confirmed by scoring embryonic lethality.

In Vitro Kinase Assays

Aurora-B^{AIR-2} and the INCENP^{ICP-1} WT and ts C terminus (amino acids 521–622) were cloned from *C. elegans* cDNA with a 6-His N-terminal tag on Aurora-B^{AIR-2} and expressed by baculovirus in SF9 insect cells. Kinase assay reactions were carried out for 1 hr at 30°C. See Supplemental Experimental Procedures for more details.

SUPPLEMENTAL INFORMATION

Supplemental Information includes Supplemental Experimental Procedures, three figures, two tables, and six movies and can be found with this article online at http://dx.doi.org/10.1016/j.devcel.2014.05.009.

AUTHOR CONTRIBUTIONS

All experiments were conceived by J.C.C. with input from T.D. and S.N.J. T.D. and S.N.J. performed the upshift experiments and live cell analysis. J.C.C. cloned the *formin^{CYK-1}(ts)* and *INCENP^{ICP-1}(ts)* alleles. J.C.C. and V.C. constructed all the strains used here. J.S. and D.R.K. did the in vitro pyrene actin assays with wt and ts formin^{CYK-1} FH1FH2C. K.L. and J.D. conducted the in vitro Aurora-B^{AIR-2}/INCENP^{ICP-1} kinase assay. A.C. sequenced *cyk-1* in the *formin^{CYK-1}(ts)* mutant. J.C.C., M.S.H., T.D., and S.N.J. wrote the manuscript.

ACKNOWLEDGMENTS

We thank all members of the Canman lab for support and advice, as well as Gregg Gundersen, Jeroen van den Berg, Yelena Zhuravlev, Sriramkumar Sundaramoorthy, Elizabeth Stone, Victoria Allen, Vanessa Hill, and Reed O'Conner for critical reading of this manuscript. We are grateful to Thomas Nguyen, Zhaoqi Li, Jeffrey Cochran, Natalia Romano Spica, Amanda Smith, Alana Ramjit, Sungkyu Oh, and Jeremy Cohen for making worm plates and buffers. We thank Jennifer Waters for microscopy consultation; Iain Cheeseman for eyelashes; Amy Maddox for WT *cyk-1* sequence information; and Bruce Bowerman, Michael Glotzer, John White, and the CGC for worm strains. We also thank Dan Focht and everyone at Bioptechs for building the Therminator. NIH R01 GM079265 to D.R.K.; ANR-09-RPDOC-005-01 and FRM AJE201112 and the Emergence program from Mairie de Paris to J.D.; NIH R01 GM105775 to M.S.H.; and NIH DP2 OD008773 to J.C.C.

Received: October 11, 2013
Revised: March 17, 2014
Accepted: May 12, 2014
Published: July 28, 2014

REFERENCES

Bastos, R.N., Penate, X., Bates, M., Hammond, D., and Barr, F.A. (2012). CYK4 inhibits Rac1-dependent PAK1 and ARHGEF7 effector pathways during cytokinesis. J. Cell Biol. *198*, 865–880.

Bishop, J.D., and Schumacher, J.M. (2002). Phosphorylation of the carboxyl terminus of inner centromere protein (INCENP) by the Aurora B Kinase stimulates Aurora B kinase activity. J. Biol. Chem. *277*, 27577–27580.

Brenner, S. (1974). The genetics of Caenorhabditis elegans. Genetics *77*, 71–94.

Burkel, B.M., Benink, H.A., Vaughan, E.M., von Dassow, G., and Bement, W.M. (2012). A Rho GTPase signal treadmill backs a contractile array. Dev. Cell *23*, 384–396.

Canman, J.C., Lewellyn, L., Laband, K., Smerdon, S.J., Desai, A., Bowerman, B., and Oegema, K. (2008). Inhibition of Rac by the GAP activity of centralspindlin is essential for cytokinesis. Science *322*, 1543–1546.

Carmena, M., Wheelock, M., Funabiki, H., and Earnshaw, W.C. (2012). The chromosomal passenger complex (CPC): from easy rider to the godfather of mitosis. Nat. Rev. Mol. Cell Biol. *13*, 789–803.

Carvalho, A., Desai, A., and Oegema, K. (2009). Structural memory in the contractile ring makes the duration of cytokinesis independent of cell size. Cell *137*, 926–937.

Collette, K.S., Petty, E.L., Golenberg, N., Bembenek, J.N., and Csankovszki, G. (2011). Different roles for Aurora B in condensin targeting during mitosis and meiosis. J. Cell Sci. *124*, 3684–3694.

D'Avino, P.P., Savoian, M.S., and Glover, D.M. (2004). Mutations in sticky lead to defective organization of the contractile ring during cytokinesis and are enhanced by Rho and suppressed by Rac. J. Cell Biol. *166*, 61–71.

de Carvalho, C.E., Zaaijer, S., Smolikov, S., Gu, Y., Schumacher, J.M., and Colaiácovo, M.P. (2008). LAB-1 antagonizes the Aurora B kinase in C. elegans. Genes Dev. *22*, 2869–2885.

Douglas, M.E., Davies, T., Joseph, N., and Mishima, M. (2010). Aurora B and 14-3-3 coordinately regulate clustering of centralspindlin during cytokinesis. Curr. Biol. *20*, 927–933.

Encalada, S.E., Martin, P.R., Phillips, J.B., Lyczak, R., Hamill, D.R., Swan, K.A., and Bowerman, B. (2000). DNA replication defects delay cell division and disrupt cell polarity in early Caenorhabditis elegans embryos. Dev. Biol. *228*, 225–238.

Fang, X., Luo, J., Nishihama, R., Wloka, C., Dravis, C., Travaglia, M., Iwase, M., Vallen, E.A., and Bi, E. (2010). Biphasic targeting and cleavage furrow ingression directed by the tail of a myosin II. J. Cell Biol. *191*, 1333–1350.

Gönczy, P., Schnabel, H., Kaletta, T., Amores, A.D., Hyman, T., and Schnabel, R. (1999). Dissection of cell division processes in the one cell stage Caenorhabditis elegans embryo by mutational analysis. J. Cell Biol. *144*, 927–946.

Green, R.A., Paluch, E., and Oegema, K. (2012). Cytokinesis in animal cells. Annu. Rev. Cell Dev. Biol. *28*, 29–58.

Green, R.A., Mayers, J.R., Wang, S., Lewellyn, L., Desai, A., Audhya, A., and Oegema, K. (2013). The midbody ring scaffolds the abscission machinery in the absence of midbody microtubules. J. Cell Biol. *203*, 505–520.

Heallen, T.R., Adams, H.P., Furuta, T., Verbrugghe, K.J., and Schumacher, J.M. (2008). An Afg2/Spaf-related Cdc48-like AAA ATPase regulates the stability and activity of the C. elegans Aurora B kinase AIR-2. Dev. Cell *15*, 603–616.

Honda, R., Körner, R., and Nigg, E.A. (2003). Exploring the functional interactions between Aurora B, INCENP, and survivin in mitosis. Mol. Biol. Cell *14*, 3325–3341.

Hu, C.K., Coughlin, M., and Mitchison, T.J. (2012). Midbody assembly and its regulation during cytokinesis. Mol. Biol. Cell *23*, 1024–1034.

Hutterer, A., Glotzer, M., and Mishima, M. (2009). Clustering of centralspindlin is essential for its accumulation to the central spindle and the midbody. Curr. Biol. *19*, 2043–2049.

Jantsch-Plunger, V., Gönczy, P., Romano, A., Schnabel, H., Hamill, D., Schnabel, R., Hyman, A.A., and Glotzer, M. (2000). CYK-4: A Rho family gtpase activating protein (GAP) required for central spindle formation and cytokinesis. J. Cell Biol. *149*, 1391–1404.

Jordan, S.N., and Canman, J.C. (2012). Rho GTPases in animal cell cytokinesis: an occupation by the one percent. Cytoskeleton (Hoboken) *69*, 919–930.

Kaitna, S., Mendoza, M., Jantsch-Plunger, V., and Glotzer, M. (2000). Incenp and an aurora-like kinase form a complex essential for chromosome segregation and efficient completion of cytokinesis. Curr. Biol. *10*, 1172–1181.

Kamasaki, T., Osumi, M., and Mabuchi, I. (2007). Three-dimensional arrangement of F-actin in the contractile ring of fission yeast. J. Cell Biol. *178*, 765–771.

Kimura, K., Tsuji, T., Takada, Y., Miki, T., and Narumiya, S. (2000). Accumulation of GTP-bound RhoA during cytokinesis and a critical role of ECT2 in this accumulation. J. Biol. Chem. *275*, 17233–17236.

Kuhn, J.R., and Pollard, T.D. (2005). Real-time measurements of actin filament polymerization by total internal reflection fluorescence microscopy. Biophys. J. *88*, 1387–1402.

Lekomtsev, S., Su, K.C., Pye, V.E., Blight, K., Sundaramoorthy, S., Takaki, T., Collinson, L.M., Cherepanov, P., Divecha, N., and Petronczki, M. (2012). Centralspindlin links the mitotic spindle to the plasma membrane during cytokinesis. Nature *492*, 276–279.

Lewellyn, L., Carvalho, A., Desai, A., Maddox, A.S., and Oegema, K. (2011). The chromosomal passenger complex and centralspindlin independently contribute to contractile ring assembly. J. Cell Biol. *193*, 155–169.

Liu, J., Maduzia, L.L., Shirayama, M., and Mello, C.C. (2010). NMY-2 maintains cellular asymmetry and cell boundaries, and promotes a SRC-dependent asymmetric cell division. Dev. Biol. *339*, 366–373.

Loria, A., Longhini, K.M., and Glotzer, M. (2012). The RhoGAP domain of CYK-4 has an essential role in RhoA activation. Curr. Biol. *22*, 213–219.

Lupas, A., Van Dyke, M., and Stock, J. (1991). Predicting coiled coils from protein sequences. Science *252*, 1162–1164.

Ma, X., Kovács, M., Conti, M.A., Wang, A., Zhang, Y., Sellers, J.R., and Adelstein, R.S. (2012). Nonmuscle myosin II exerts tension but does not translocate actin in vertebrate cytokinesis. Proc. Natl. Acad. Sci. USA *109*, 4509–4514.

Mendes Pinto, I., Rubinstein, B., Kucharavy, A., Unruh, J.R., and Li, R. (2012). Actin depolymerization drives actomyosin ring contraction during budding yeast cytokinesis. Dev. Cell *22*, 1247–1260.

Mishima, M., Kaitna, S., and Glotzer, M. (2002). Central spindle assembly and cytokinesis require a kinesin-like protein/RhoGAP complex with microtubule bundling activity. Dev. Cell *2*, 41–54.

Mishra, M., Kashiwazaki, J., Takagi, T., Srinivasan, R., Huang, Y., Balasubramanian, M.K., and Mabuchi, I. (2013). In vitro contraction of cytokinetic ring depends on myosin II but not on actin dynamics. Nat. Cell Biol. *15*, 853–859.

Murthy, K., and Wadsworth, P. (2005). Myosin-II-dependent localization and dynamics of F-actin during cytokinesis. Curr. Biol. *15*, 724–731.

Neidt, E.M., Skau, C.T., and Kovar, D.R. (2008). The cytokinesis formins from the nematode worm and fission yeast differentially mediate actin filament assembly. J. Biol. Chem. *283*, 23872–23883.

Nishimura, K., Fukagawa, T., Takisawa, H., Kakimoto, T., and Kanemaki, M. (2009). An auxin-based degron system for the rapid depletion of proteins in nonplant cells. Nat. Methods *6*, 917–922.

Nunes Bastos, R., Gandhi, S.R., Baron, R.D., Gruneberg, U., Nigg, E.A., and Barr, F.A. (2013). Aurora B suppresses microtubule dynamics and limits central spindle size by locally activating KIF4A. J. Cell Biol. *202*, 605–621.

O'Connell, K.F., Leys, C.M., and White, J.G. (1998). A genetic screen for temperature-sensitive cell-division mutants of Caenorhabditis elegans. Genetics *149*, 1303–1321.

Otomo, T., Tomchick, D.R., Otomo, C., Panchal, S.C., Machius, M., and Rosen, M.K. (2005). Structural basis of actin filament nucleation and processive capping by a formin homology 2 domain. Nature *433*, 488–494.

Pavicic-Kaltenbrunner, V., Mishima, M., and Glotzer, M. (2007). Cooperative assembly of CYK-4/MgcRacGAP and ZEN-4/MKLP1 to form the centralspindlin complex. Mol. Biol. Cell *18*, 4992–5003.

Pelham, R.J., and Chang, F. (2002). Actin dynamics in the contractile ring during cytokinesis in fission yeast. Nature *419*, 82–86.

Proctor, S.A., Minc, N., Boudaoud, A., and Chang, F. (2012). Contributions of turgor pressure, the contractile ring, and septum assembly to forces in cytokinesis in fission yeast. Curr. Biol. *22*, 1601–1608.

Reddien, P.W., and Horvitz, H.R. (2000). CED-2/CrkII and CED-10/Rac control phagocytosis and cell migration in Caenorhabditis elegans. Nat. Cell Biol. *2*, 131–136.

Reichl, E.M., Ren, Y., Morphew, M.K., Delannoy, M., Effler, J.C., Girard, K.D., Divi, S., Iglesias, P.A., Kuo, S.C., and Robinson, D.N. (2008). Interactions between myosin and actin crosslinkers control cytokinesis contractility dynamics and mechanics. Curr. Biol. *18*, 471–480.

Robinson, M.S., Sahlender, D.A., and Foster, S.D. (2010). Rapid inactivation of proteins by rapamycin-induced rerouting to mitochondria. Dev. Cell *18*, 324–331.

Schroeder, T.E. (1972). The contractile ring. II. Determining its brief existence, volumetric changes, and vital role in cleaving Arbacia eggs. J. Cell Biol. *53*, 419–434.

Severson, A.F., Hamill, D.R., Carter, J.C., Schumacher, J., and Bowerman, B. (2000). The aurora-related kinase AIR-2 recruits ZEN-4/CeMKLP1 to the mitotic spindle at metaphase and is required for cytokinesis. Curr. Biol. *10*, 1162–1171.

Skop, A.R., Liu, H., Yates, J., 3rd, Meyer, B.J., and Heald, R. (2004). Dissection of the mammalian midbody proteome reveals conserved cytokinesis mechanisms. Science *305*, 61–66.

Spudich, J.A., and Watt, S. (1971). The regulation of rabbit skeletal muscle contraction. I. Biochemical studies of the interaction of the tropomyosin-troponin complex with actin and the proteolytic fragments of myosin. J. Biol. Chem. *246*, 4866–4871.

Su, K.C., Takaki, T., and Petronczki, M. (2011). Targeting of the RhoGEF Ect2 to the equatorial membrane controls cleavage furrow formation during cytokinesis. Dev. Cell *21*, 1104–1115.

Tama, F., Feig, M., Liu, J., Brooks, C.L., 3rd, and Taylor, K.A. (2005). The requirement for mechanical coupling between head and S2 domains in smooth

muscle myosin ATPase regulation and its implications for dimeric motor function. J. Mol. Biol. *345*, 837–854.

Timmons, L., Court, D.L., and Fire, A. (2001). Ingestion of bacterially expressed dsRNAs can produce specific and potent genetic interference in Caenorhabditis elegans. Gene *263*, 103–112.

Tse, Y.C., Werner, M., Longhini, K.M., Labbe, J.C., Goldstein, B., and Glotzer, M. (2012). RhoA activation during polarization and cytokinesis of the early Caenorhabditis elegans embryo is differentially dependent on NOP-1 and CYK-4. Mol. Biol. Cell *23*, 4020–4031.

Uehara, R., Tsukada, Y., Kamasaki, T., Poser, I., Yoda, K., Gerlich, D.W., and Goshima, G. (2013). Aurora B and Kif2A control microtubule length for assembly of a functional central spindle during anaphase. J. Cell Biol. *202*, 623–636.

Verbrugghe, K.J., and White, J.G. (2004). SPD-1 is required for the formation of the spindle midzone but is not essential for the completion of cytokinesis in C. elegans embryos. Curr. Biol. *14*, 1755–1760.

Xu, Z., Ogawa, H., Vagnarelli, P., Bergmann, J.H., Hudson, D.F., Ruchaud, S., Fukagawa, T., Earnshaw, W.C., and Samejima, K. (2009). INCENP-aurora B interactions modulate kinase activity and chromosome passenger complex localization. J. Cell Biol. *187*, 637–653.

Xu, Z., Vagnarelli, P., Ogawa, H., Samejima, K., and Earnshaw, W.C. (2010). Gradient of increasing Aurora B kinase activity is required for cells to execute mitosis. J. Biol. Chem. *285*, 40163–40170.

Yoshizaki, H., Ohba, Y., Parrini, M.C., Dulyaninova, N.G., Bresnick, A.R., Mochizuki, N., and Matsuda, M. (2004). Cell type-specific regulation of RhoA activity during cytokinesis. J. Biol. Chem. *279*, 44756–44762.

Yüce, O., Piekny, A., and Glotzer, M. (2005). An ECT2-centralspindlin complex regulates the localization and function of RhoA. J. Cell Biol. *170*, 571–582.

Zhao, W.M., and Fang, G. (2005). MgcRacGAP controls the assembly of the contractile ring and the initiation of cytokinesis. Proc. Natl. Acad. Sci. USA *102*, 13158–13163.

Zumdieck, A., Kruse, K., Bringmann, H., Hyman, A.A., and Jülicher, F. (2007). Stress generation and filament turnover during actin ring constriction. PLoS ONE *2*, e696.